Construction of an efficient editing system for forest tree genomes based on a visual screening marker in Eucalyptus urophylla × Eucalyptus grandis

Ming Su
Guangdong University of Petrochemical Technology
Xinlin Wu
Guangdong University of Petrochemical Technology
Zechen Wang
Guangdong University of Petrochemical Technology
Limei Li
Guangdong University of Petrochemical Technology
lejun Ouyang
ouyanglejun@gdupt.edu.cn
Guangdong University of Petrochemical Technology
Chao Shen
Guangdong University of Petrochemical Technology

Research Article

Keywords: Eucalyptus urophylla × Eucalyptus grandis, screening marker, CRISPR/Cas9, C4H

Posted Date: January 15th, 2024

DOI: https://doi.org/10.21203/rs.3.rs-3844840/v1

Additional Declarations: No competing interests reported.

Abstract

In this study, The clustered regularly interspaced short palindromic repeats (CRISPR)/CRISPR-associated protein 9 (Cas9) technology for genome editing was used to develop an efficient gene editing system for *Eucalyptus urophylla × Eucalyptus grandis* and generate a new *Eucalyptus* germplasm with reduced lignin contents in the pulp for environmental sustainability in papermaking. By targeting the Cinnamate-4-hydroxylase (C4H) gene in *E. urophylla × E. grandis*, the recombinant plasmid pHEE401E-*35S-RUBY-EuC4H* was constructed through homologous recombination. This plasmid was then transformed into *E. urophylla × E. grandis* callus tissue. Using the *RUBY* gene as a marker, positive transformants were screened based on the callus tissue phenotype. Subsequent polymerase chain reaction and sequencing confirmed the successful creation of mutants with a significantly edited *EuC4H* gene. The method used in this study for identifying positive transformants with a visually screened marker gene offers a valuable framework and guidance for genetically improving and establishing an efficient gene editing system in *Eucalyptus*.

1 Introduction

Eucalyptus are a genus within the Myrtle family (Myrtaceae) (Wei Hong, et al, 2008) and are one of the top three fast-growing trees globally, serving as a key raw material for the pulp and paper industry Tao Liu and Yaojian Xie, 2020. Their wide applications can be attributed to a variety of advantages, including short growth periods, high wood density, long fibers, and high yield. The genus has been introduced in over 100 countries Qiheng Tang and Yongping Chen, 2020. In China, the history of *Eucalyptus* dates back over 130 years, with substantial progress made in its cultivation, particularly in the southeast coastal regions of the Guangxi and Guangdong provinces Guoqin Huang and Qiguo Zhao, 2014. At present, it has become one of the most important commercial forest species in China and is extensively used in the production of pulp for paper and wood-based panel manufacturing Yaojian Xie, 2018. The genus plays an instrumental role in upholding China's timber security.

Lignin predominantly consists of three types: syringyl lignin (S lignin), guaiacyl lignin (G lignin), and hydroxy-phenyl lignin (H lignin); it is the second most abundant amorphous natural polymer in plants after cellulose (Editorial Board of Forest Industry Volume China Agricultural Encyclopedia Editorial Department, 1993). In *Eucalyptus*, a dicotyledonous angiosperm, lignin primarily consists of an approximately equal amount of G and S lignins, with a minor amount of H lignin Yitong Liu, 2017; He-xiang Feng and Yi Tu, 2018. The lignin biosynthetic pathway is currently believed to include the shikimic acid pathway, phenylpropanoid metabolic pathway, and other specific pathways Bowen Chen, 2017. Phenylalanine is the substrate for lignin biosynthesis, and the phenylpropanoid pathway is critical in generating plant secondary metabolites, with all components of known lignin polymers produced or derived from this pathway (Vanholme R, et al, 2019). Cinnamate-4-hydroxylase (C4H), an essential enzyme in this pathway, is a conserved cytochrome P450 (CYP) monooxygenase in the CYP73 family (Li W, et al, 2016). Regulation of C4H activity affects the overall lignin content in plants. Yan et al. showed an increase in lignin accumulation and enhanced defense against pests and diseases in *nicotiana*

benthamiana plants overexpressing the *C4H* gene (Yan Q, et al, 2019). In contrast, suppression of *C4H* expression led to a significant decrease in the lignin content in tobacco stems (Blount JW, et al, 2000). Simmons et al. reported that *Arabidopsis* mutants of the *C4H* gene displayed phenotypes such as pollen sterility, dwarfism, and a significant reduction in the lignin content compared with those of wild-type plants (Simmons CR, et al, 2001). Sykes et al. used RNA interference to inhibit *C4H* activity in *Eucalyptus grandis* and observed an approximate 30% decrease in the total lignin and a reduced S/G ratio (Sykes RW, et al, 2015). Franke et al. found that using the *C4H* promoter to drive *ferulate 5-hydroxylase* (*F5H)* gene expression increased the synthesis of S lignin monomers in tobacco stems, whereas the *35S* promoter further enhanced S lignin overexpression in petioles. Similar phenotypes were observed in *populus tremula × alba* containing the *C4H-F5H* transgene, suggesting there was stem-specific expression of the *C4H* promoter (Franke R, et al, 2000).

The *RUBY* reporter system is a novel, convenient system that allows the detection of the reporter gene by the naked eye under natural light. Independently developed by our group, this system is based on the principle that the conversion of tyrosine into betanin, which gives a vivid red color that is visible under natural light, requires as few as three enzymatic reactions (Polturak, Aharoni, 2019). The approach offers considerable advantages over traditional reporter genes, with *in situ* observations eliminating the needs for additional instruments and sample preprocessing for screening, rendering the process fast and convenient. The color change in the transformed callus tissue allows for the rapid screening of positive transformants, which substantially enhances the efficiency of transformant identification (Tanaka Y, et al, 1974; HE, et al, 2020). Using *RUBY* as a marker for the visual screening of positive transformants, this approach mitigates the issues of low screening efficiency and high false-positive rate associated with the antibiotic screening of *Eucalyptus* chimeric transformants.

In this study, *E. urophylla × E. grandis* served as the experimental subject. Using CRISPR/Cas9 gene editing technology, a site-specific editing vector targeting the *EuC4H* gene was constructed. Post-transformation, the expression of *RUBY* was used to identify positive transformants, which were further confirmed through polymerase chain reaction (PCR) and sequencing to verify editing in the *C4H* gene. This study offers valuable insights and guidance for the future development of an efficient and precise site-specific editing system in *Eucalyptus*, as well as for the targeted breeding of new, environmentally friendly *E. urophylla × E. grandis* germplasms suitable for pulp production.

2 Materials and Methods

2.1 Test materials

The aseptic seedlings of *E. urophylla × E. grandis* were obtained from the Zhanjiang Academy of Forestry in Guangdong Province, China. Competent cells of the *Escherichia coli* strain DH5α and *Agrobacterium tumefaciens* strain GV3101 were acquired from Beijing BM Biomed Co., Ltd in Beijing China. The plasmids pHDE, pCBC, and pHEE401E-EC2-Cas9 were stored in an ultra-low temperature freezer in the

laboratory. The plasmid template containing the *RUBY* reporter gene was kindly provided by the Nanjing Agricultural University and Professor Yu Bing in Nanjing, China.

2.2 Main test reagents

The Easy pure quick gel extraction kit, TransZol up plus kit, TransStart tip green quantitative PCR (qPCR) supermix, and TransScript one-step gDNA removal and cDNA synthesis supermix were purchased from Beijing TransGen Biotech Co., Ltd in Beijing China. The Ezup spin column super plant genomic DNA extraction kit is a product of Sangon Biotech (Shanghai) Co., Ltd in Shanghai China.

2.3 Construction of the pHEE401E-*35S-RUBY-EuC4H* vector

2.3.1 Primer design

The *C4H* sequence of *E. grandis* (XM_010034641) was retrieved from the National Center for Biotechnology Information (NCBI) and BLAST alignment was performed against the whole genome of *E. urophylla × E. grandis* to identify the *EuC4H* (Eug10G0172600.1) sequence. Primers containing target sequences were designed using the online tool CRISPR direct (http://crispr.dbcls.jp/) for plasmid construction. Other primers were designed with Primer3 online (Table 1) and synthesized by Sangon Biotech (Shanghai) Co., Ltd in China.

[Insert Table 1 here]

2.3.2 Construction of the pHEE401E-*35S-RUBY* vector

(1) Amplification of the *35S* promoter and *RUBY* target fragment

The *35S* promoter fragment was amplified from the pHDE plasmid using R*35S*-F and R*35S*-R as the upstream and downstream primers, respectively. The *RUBY* target fragment was amplified from the *DR5-RUBY* plasmid using R*RUBY*-F and R*RUBY*-R as primers. The PCR program used is shown in Table 2. Following electrophoresis, the corresponding PCR products were purified and recovered.

[Insert Table 2 here]

(2) Fusion PCR amplification of the *35S-RUBY* fragment

The purified *35S* promoter and *RUBY* fragments were used as templates for the overlap extension PCR with R*35S*-F and R*RUBY*-R as the primers. The PCR program is the same as that described previously (Table 2). After electrophoresis, the PCR products were purified and recovered.

(3) Restriction digestion and homologous recombination of the pHEE401E-*35S-Cas9* plasmid

The pHEE401E-*35S-Cas9* plasmid (stored in the laboratory) was digested with the *Mfe* I restriction enzyme. The purified *35S-RUBY* target fragment underwent homologous recombination with the digestion product to construct the pHEE401E-*35S-RUBY* plasmid.

(4) Transformation of the recombinant plasmid into *E. coli* competent cells and the identification of transformants

The recombinant plasmid was transformed into *DH5a* competent cells via heat shock. Transformants were identified using bacterial and plasmid PCR. Positive clones were sequenced to confirm the successful construction of the pHEE401E-*35S-RUBY* plasmid.

2.3.3 Construction of the pHEE401E-*35S-RUBY-EuC4H* vector

(1) Amplification of sgRNA fragments containing two specific target sites

Using the pCBC plasmid stored in the laboratory as a template, PCR amplification of the corresponding target sites was performed using the *EuC4H*-gF/*EuC4H-gR* primers. The PCR program is shown in Table 3. Following electrophoresis, the corresponding PCR products were purified and recovered.

(2) Restriction digestion and homologous recombination of the pHEE401E-*35S-RUBY* plasmid

The pHEE401E-*35S-RUBY* plasmid was digested with the *Bsa* I restriction enzyme, and recombinational cloning with the gRNA fragment was performed. The reaction mixture contained 5 μL recombinase, 2.5 μL linear vector, and 2.5 μL insert fragment, and was incubated in a 55°C water bath for 15 min.

(3) Transformation of the recombinant plasmid into *E. coli* competent cells and the identification of transformants

The recombinant plasmid was introduced into competent *E. coli* cells using the heat shock method. Positive clones were identified using bacterial PCR, followed by culture expansion and extraction of the recombinant plasmid. Plasmid PCR was conducted to identify transformants, and the recombinant plasmid was then subjected to sequencing.

(4) Preparation of the engineered bacterial culture

Positive recombinant plasmid clones confirmed using sequencing were transformed into *A. tumefaciens* competent cells. Single colonies resistant to rifampicin and kanamycin were selected for culturing. These bacterial cultures were then used as templates for PCR identification using *EuC4H*-F/*EuC4H*-R as primers. *Agrobacterium tumefaciens* colonies with the desired band size were selected for further culturing at 28°C and 200 rpm for 20 h to prepare the engineered bacterial cultures.

[Insert Table 3 here]

2.3.4 Transformation and identification of the pHEE401E-*35S-RUBY-EuC4H* plasmid

Stem segments without buds were cut into 3–6 mm pieces from aseptic seedlings of *E. urophylla × E. grandis* and used as explants. These were cultured on a callus induction medium at 24°C in the dark for one week. The explants were then immersed in 100 mL of transformation solution and subjected to 40 kHz ultrasonication for 1 min. A fresh bacterial culture of *A. tumefaciens* carrying the pHEE401E-*35S*-*RUBY*-*C4H* plasmid was centrifuged at 5,000 rpm for 1 min, and the resulting pellet was resuspended in the transformation solution with the callus tissue. This mixture was incubated on a shaker at 50 rpm and 28°C in the dark for 3 h. Subsequently, the treated callus tissue was transferred back to the callus induction medium and co-cultured in the dark at 22°C for one week. The callus tissue was then transferred to a bud induction medium containing 300 mg/L cefotaxime sodium and further cultured in the dark for another week before being cultured in the light. The medium was changed biweekly, and the growth of the callus tissue and the expression of *RUBY* were monitored.

Transformed callus tissue exhibiting red coloration was selected and cut, and the DNA was extracted to serve as a template. PCR amplification was performed using *RUBY*-GT1/*RUBY*-GT2 primers to confirm the integration of the marker gene *RUBY* into the callus tissue. Then, using *EuC4H*-GT1/*EuC4H*-GT2 primers, PCR products were analyzed by electrophoresis to verify the expected band sizes. If a smaller band was observed, it was excised and sequenced, and the sequencing results were compared with the expected sequence to confirm the successful editing of the *EuC4H* gene.

2.3.5 Correlation between the extent of red coloration and RUBY gene expression in the callus tissue of E. urophylla × E. grandis

A total of 100 mg samples from four different types of callus tissues, each showing varying degrees of red color indicative of various expressions of the *RUBY* gene, were weighed and used for RNA extraction. RNA was extracted using the TransZol Up Plus Kit Total RNA Extraction Kit from Beijing TransGen Biotech Co., Ltd. For reverse transcription, the TransScript One-Step gDNA Removal and cDNA Synthesis SuperMix kit (TransGen Biotech) was used to synthesize the cDNA.

The actin gene of *E. urophylla × E. grandis* (XM_010038187.3) served as an internal control for the qPCR experiments. The relationship between the varying degrees of red coloration in the callus tissues as phenotypes and *RUBY* gene expression was assessed through real-time fluorescence qPCR. Primer sequences are listed in Table 1.

The TransStart Tip Green qPCR SuperMix kit from TransGen Biotech was used for the qPCR experiments. The total qPCR reaction volume was 20 μL and consisted of 0.4 μL each of the upstream (F) and downstream (R) primers at a concentration of 20 μM after dilution, 10 μL of the super mix, 0.4 μL of dye, 1 μL of the sample, and 7.8 μL of nuclease-free water. Reaction conditions were as follows: initial denaturation at 94°C for 4 min 30 s, followed by 40 cycles of 1) 94°C for 5 s, 2) 56°C for 15 s, and 3) 72°C for 10 s. Each sample in the qPCR reaction was set up in quadruplicate. Relative gene expression was calculated using the $2^{-\Delta\Delta Ct}$ method, analyzed and plotted.

3 Results

3.1 Construction of the pHEE401E-*35S-RUBY* vector

The *35S* promoter and *RUBY* target fragment were amplified using pHDE plasmid and DR5-RUBY plasmid as templates, respectively. Electrophoresis after the amplification showed that the *35S* promoter (Fig. 1A) and *RUBY* target bands (Fig. 1B) were consistent with the expected size. The *35S* promoter and *RUBY* bands were then excised from the gel for recovery.

The recovered *35S* promoter and *RUBY* bands were joined using overlap extension PCR. The size of the joined fragment was consistent with the expected band size, as shown in Fig. 1C, and the target band was recovered.

The recovered *35S-RUBY* target band was recombined with the *Mfe* I digested pHEE401E-*35S-Cas9* plasmid through homologous recombination. After transformation into the *E. coli DH5α* competent cells, verification with bacterial and plasmid PCR (Fig. 1D, E) indicated successful construction of the pHEE401E-*35S-RUBY* vector. The vector structure is shown in Fig. 2.

[Insert Fig. 1 here]

[Insert Fig. 2 here]

3.2 Construction of the pHEE401E-*35S-RUBY-EuC4H* vector

Using the pCBC plasmid as a template, sgRNA was amplified by PCR, yielding a product with a size between 500 and 750 bp, consistent with the expected size (Fig. 3A). The PCR product was gel-excised and purified, and used for assembling the recombinant plasmid. The *Bsa* I digestion of the pHEE401E-*35S-RUBY* plasmid resulted in a noticeable difference in the band size before and after digestion, yielding linear plasmids with bright bands and indicating complete digestion (Fig. 3B).

The recovered purified fragment and linear vector were then assembled through homologous recombination. The recombinant plasmid was transformed into *E. coli* via heat shock, followed by resistance screening. Single resistant colonies were selected for subsequent culture. Bacterial PCR results revealed band sizes between 500 and 750 bp (Fig. 3C). The bands matched the expected size and indicated a high ratio of positive clones. After the expanded culture of bacterial colonies with good quality bands, plasmid extraction and PCR verification of the plasmids were performed, and band sizes matched the expectations; the results are shown in Fig. 3D. Sequencing analysis confirmed the successful construction of the pHEE401E-*35S-RUBY-EuC4H* vector; the structure of the recombinant plasmid is shown in Fig. 4. It was then transformed into *A. tumefaciens* competent cells using the heat shock method to prepare the engineered bacterial culture.

[Insert Fig. 3 here]

[Insert Fig. 4 here]

3.3 Transformation and identification of the pHEE401E-*35S-RUBY-EuC4H* vector

After a period of culture in light post-transformation, most of the *E. urophylla × E. grandis* callus tissue exhibited red coloration on the surface (Fig. 5A). Upon continued culture until budding (Fig. 5B), parts of the leaves turned red, indicating partial expression of *RUBY* in the plant tissues.

Following the culture of the callus tissue in light, no significant differences in external characteristics, aside from varying degrees of redness, were observed (Fig. 5A). The callus tissues that turned red post-transformation were divided into four groups (Fig. 6A). RNA was extracted from each group for quality assessment via electrophoresis. Slight trailing in the bands indicative of diffusion was observed. The brightness of the 28S rRNA band was approximately twice that of the 18S, demonstrating good integrity of the samples and that they met the requirements for subsequent experiments (Fig. 6B).

GraphPad Prism trial version was used to analyze the exported data containing Ct values. Using Sample a as the reference, a t-test was conducted for the significance analysis of differential expression; the results of which are presented using a histogram (Fig. 6C). A positive correlation between the expression level of *RUBY* and degree of redness in the phenotype of the *E. urophylla × E. grandis* callus tissue was observed, confirming *RUBY* as an effective marker gene for screening.

[Insert Fig. 5 here]

[Insert Fig. 6 here]

DNA from the red callus tissue was used as a template to identify the marker gene *RUBY*. The bands of the PCR products were approximately 750 bp in size (Fig. 6D), consistent with the expected size and suggesting successful integration of *RUBY* into the callus tissue at a high transformation rate. Gene editing results were then verified using the *EuC4H* identification primers. As shown in Fig. 6E, Lane 3 exhibited two bands, with the smaller band between 250 and 500 bp, consistent with the expected size post-editing. This smaller band was recovered for sequencing, and the sequencing results were compared with the expected sequence (Fig. 7A). The analysis revealed overlapping peaks starting from 125 bp. Using the Sanger Sequencing Check Advanced plugin from TBtools, with the Gap Extension parameter set to 0 and others at default settings, two allelic sequences, S1 and S2, were derived after separating the peaks. A comparison of these two allelic sequences with the reference sequence (Fig. 7B) revealed insertions, deletions, and partial base mutations in the *EuC4H* gene, not only between but also beyond the two target sites, preliminarily confirming the successful editing of the target gene.

[Insert Fig. 7 here]

4 Discussion

Currently, traditional *Agrobacterium*-mediated transformation and biolistic (gene gun) methods are primarily used for gene delivery into plant cells. The efficiency of these transformations generally depends on the genotype and species of the plant, limiting their applicability to a select number of species and genotypes, and an extended period of tissue culture is often required to cultivate complete plants (Ji X, Yang B, Wang D, 2020). A robust and efficient genetic transformation system remains elusive for most woody plants. In most systems, callus tissues serve as the transformation recipient, and selecting the appropriate type and dosage of antibiotics is crucial in developing these systems. Antibiotics such as kanamycin and hygromycin B are commonly used for selecting positive transformants, yet their toxicity to most plants is relatively high. The reliance on antibiotic selection for transformed chimeras poses significant challenges in screening and identification owing to low efficiency and a high rate of false positives.

Eucalyptus urophylla × E. grandis is a rapidly growing hybrid of *E. urophylla* and *E. grandis.* Its large and complex genome complicates the acquisition of homozygous transgenic and gene-edited plants. A significant challenge in using callus tissue for genetic transformation in this species is the identification of positive transformants, which is also crucial for enhancing screening efficiency. In this study, the traditional *Agrobacterium*-mediated approach was used to deliver the recombinant plasmids. Despite a brief experimental cycle, straightforward approach, and relatively high transformation rate, the transformed explants obtained by tissue culture frequently showed chimerism, which made subsequent genotyping highly laborious and inefficient. Additionally, the probability of obtaining homozygous gene-edited plants was also low. Therefore, it is crucial to focus on developing and applying new methods for rapidly acquiring positive transformants. This will promote basic and applied plant research and fulfill increasing public demand for new germplasms with superior traits.

As a reporter gene, *RUBY* allows for the visual screening of transgenic plants, and in our study, we identified several causes for false positives in the actual tissue culturing of *E. urophylla × E. grandis*. First, the inherent characteristics of the species contributed to the issue. As a woody plant abundant in phenolic substances, *E. urophylla × E. grandis* is prone to browning during tissue culture (Gang Chen, 2017). Furthermore, the accumulation of certain secondary metabolites, such as anthocyanins Min Su, et al, 2023, can mimic the color of *RUBY*. Additionally, our observations revealed that certain explants displayed a reddish-brown color before inoculation with *A. tumefaciens*. Upon reviewing the literature, we speculated that false positives could have resulted from the integration of coniferol into lignin polymers, which turned the stems of *E. urophylla × E. grandis* red (Stewart D, et al, 1997). These factors could all potentially disrupt the visual screening process. Moreover, we observed issues inherent to *RUBY* itself. In our extended tissue culture of *E. urophylla × E. grandis*, we noted that callus tissues exhibited widespread reddening during initial light exposure post-*Agrobacterium* transformation, with this red coloration fading over time during the middle and later stages of tissue culture. Therefore, we speculated that the stability of *RUBY* was compromised under prolonged light exposure, resulting in a decline of the red phenotype. Additionally, callus tissues that initially turned red post-bud formation showed a specific pattern: red buds with larger and deeper redness on the leaves correlated with a higher likelihood of these buds ceasing growth and eventually dying. We thus hypothesized that overexpression of *RUBY* in

regenerated *E. urophylla × E. grandis* buds could have negatively impact the buds owing to secondary metabolites. Alternatively, the expression of betanin could have interfered with chloroplast growth and development in the leaves, thereby affecting chlorophyll synthesis, which ultimately hindered plant growth.

Declarations

Acknowledgements This research was supported by The National Natural Science Foundation of China (32071780); the Science and Technology Tackle Key Problemof Guangdong Province (2021S0074 2022DZXHT072 2023S018087).

Author contributions lejun Ouyang, Chao Shen conceived and designed the experiments; Min Su, Xinlin Wu, Limei Li performed the experiments and analyzed the data; Min Su wrote the paper.

Conflict of interest No competing or conflict of interests declared by all the authors.

Ethical approval This study did not involve human participants or animals.

References

1. Blount JW, Korth KL, Masoud SA, et al. Altering Expression of Cinnamic Acid 4-hydroxylase in Transgenic Plants Provides Evidence for a Feedback Loop at the Entry Point Into the Phenylpropanoid Pathway[J]. *Plant Physiology (bethesda)*, 2000, 122(1): 107-116.
2. Bowen Chen. Cloning of key genes involved in lignin monomer biosynthesis from Eucalyptusurophylla and transformation in tobacco[D]. Beijing Forestry University, 2017
3. Editorial Board of Forest Industry Volume China Agricultural Encyclopedia Editorial Department.China Agricultural Encyclopedia Forest Industry Volume [M] : Agricultural Publishing House, 1993.
4. Franke R, Mcmichael CM, Meyer K, et al. Modified Lignin in Tobacco and Poplar Plants Over-expressing the *Arabidopsis* Gene Encoding Ferulate 5-hydroxylase[J]. *The Plant Journal : for Cell and Molecular Biology*, 2000, 22(3): 223-234.
5. Gang Chen. Common Problems and Countermeasures in Rapid Propagation Technology of Forest Tissue Culture [J]. *Protection Forest Science and Technology*, 2017, (4): 100-102.
6. Guoqin Huang, Qiguo Zhao. The history, status quo, ecological problems and countermeasures of Eucalyptus plantations in Guangxi [J]. *Acta Ecologica Sinica*, 2014, 34(18): 5142-5152. doi:10.5846/stxb201405100943
7. He Y, Zhang T, Sun H, et al. A reporter for noninvasively monitoring gene expression and plant transformation[J]. *Hortic Res*, 2020, 7(1): 152.
8. He-xiang Feng, Yi Tu. Research on Lignin Biosynthesis [J]. *Journal of Qingdao University(Natural Science Edition)*, 2018, 31(1): 46-54. doi:10.3969/j.issn.1006-1037.2018.02.10

9. Ji X, Yang B, Wang D. Achieving Plant Genome Editing while Bypassing Tissue Culture.[J]. *Trends Plant Sci*, 2020, 25(5): 427-429.
10. Min Su, Yamei Liu, Limei Li, et al. Metabolomics analysis and differential expression of related genes in different callus of *Eucalyptus urophylla × E. grandis* [J]. *Plant Phusiology Journal*, 2023, 59(5): 943-953.
11. Polturak G, Aharoni A. Advances and future directions in betalain metabolic engineering[J]. *New Phytol*, 2019, 224(4): 1472-1478.
12. Qiheng Tang, Yongping Chen. Status Quo and Prospect of Wood Processing and Utilization of Eucalyptus in China and Abroad. [J]. *China Wood-Based Panels*, 2020, 27(6): 18-21.
13. Ruben Vanholme, Barbara De Meester, John Ralph, et al. Lignin biosynthesis and its integration into metabolism[J]. *Current Opinion in Biotechnology*, 2019: 230-239.
14. Simmons CR, Grant S, Altier DJ, et al. Maize Rhm1 Resistance to Bipolaris Maydis Is Associated with Few Differences in Pathogenesis-related Proteins and Global Mrna Profiles[J]. *Molecular Plant-microbe Interactions*, 2001, 14(8): 947-954.
15. Stewart D, Yahiaoui N, Mcdougall GJ, et al. Fourier-transform Infrared and Raman Spectroscopic Evidence for the Incorporation of Cinnamaldehydes Into the Lignin of Transgenic Tobacco (*nicotiana Tabacum L.*) Plants with Reduced Expression of Cinnamyl Alcohol Dehydrogenase[J]. *Planta*, 1997, 201(3): 311-318.
16. Sykes RW, Gjersing EL, Foutz K, et al. Down-regulation of P-coumaroyl Quinate/shikimate 3'-hydroxylase (c3'h) and Cinnamate 4-hydroxylase (c4h) Genes in the Lignin Biosynthetic Pathway of *Eucalyptus Urophylla × E. Grandis* Leads to Improved Sugar Release[J]. B*iotechnology for Biofuels*, 2015, 8(1): 128-128.
17. Tanaka Y, Kojima M, Uritani I, et al. Properties, Development and Cellular-localization of Cinnamic Acid 4-hydroxylase in Cut-injured Sweet Potato[J]. *Plant and Cell Physiology*, 1974, (5): 843-854.
18. Tao Liu, Yaojian Xie. Studies on the Causes of Rapid Development of Eucalyptus Plantations in China [J]. *Eucalypt Science & Technology*, 2020, 37(4): 38-47. doi:10.13987/j.cnki.askj.2020.04.07
19. Wei Hong, Han Lin, Can Chen, et al. Study on the δ13C value in different Eucalyptus species [J]. *Journal of Fujian College of Forestry*, 2008, (3): 289-293. doi:10.3969/j.issn.1001-389X.2008.03.001
20. Wei Li, Lixia Yang, Liangzhen Jiang, et al. Molecular cloning and functional characterization of a cinnamate 4-hydroxylase-encoding gene from Camptotheca acuminata[J]. *Acta Physiologiae Plantarum*, 2016, 38(11): 1-9.
21. Yan Q, Si J, Cui X, et al. The Soybean Cinnamate 4-hydroxylase Gene Gmc4h1 Contributes Positively to Plant Defense Via Increasing Lignin Content[J]. *Springe*r, 2019, 88(2): 139-141.
22. Yaojian Xie. Analysis of China's Wood Resource Security and the Contributions of Eucalyptus Plantation [J]. *Eucalypt Science & Technology*, 2018, 35(4): 3-6. doi:10.3969/j.issn.1674-3172.2018.04.002
23. Yitong Liu. Analysis of enzymatic properties of ferulic acid esterase from Clostridium thermocellum and construction of its high-efficiency plant expression vector [D]. Jiangsu University, 2017

Tables

Table 1 Primer design related to *E.urophylla × E.grandis*

Primer name	Primer sequence（5'→3'）	Purpose	Length
EuC4H-gF	ctagagtcgaagtagtgattgCATATATGGGCTCGAGAAG gttttagagctagaaatagc	Constructed plasmids	592bp
EuC4H-gR	tgctatttctagctctaaaacACCTATGAATCGAACTCGT caatcactacttcgactcta		
R*35S*-F	TAATGCATTTTATGACTTGCAACATGGTGGA GCACGACAC		462bp
R*35S*-R	GCGAGGGTCGCATGATCCATCGTGTCCTCT CCAAATGAAA		
R*RUBY*-F	TTTCATTTGGAGAGGACACGATGGATCAT GCGACCCTCG		3957bp
R*RUBY*-F	GAATTCGTTGTCAATCAATTTCACTATCACTG GAGGCTTG		
EuC4H-GT1	TATCATCGAAAATCGCGGCGG	Identification primers	736bp
EuC4H-GT2	ACCTCTCGAAAAATTGCTTGCC		
RUBY-GT1	CTCACAACTCCGCTCAACGC		725bp
RUBY-GT2	GAGTCCGGCTCTTTGAGGCT		
RUBY-qF	CGCCACACTCCTCCAGTTCTTC	qPCR primers	_
RUBY-qR	CGTCCTCGCCGTTCATCATCTT		
EuActin-F	GCACCGCCAGAGAGGAAATA		
EuActin-R	GAAGCACTTCCTGTGGACGA		

Table 2 PCR amplification procedure of pHEE401E-*35S-RUBY* vector

Temperature	Step	time
98℃	Initialization	2min
98℃	Denaturation	10 s
58℃	Annealing	15 s
72℃	Elongation	5 s/kb

Table 3 PCR reaction procedure setting

Temperature	Step	Time
94℃	Initialization	5 min
94℃	Denaturation	30 s
56℃	Annealing	30 s
72℃	Extension	60 s/kb
72℃	Complete extension	7 min

Figures

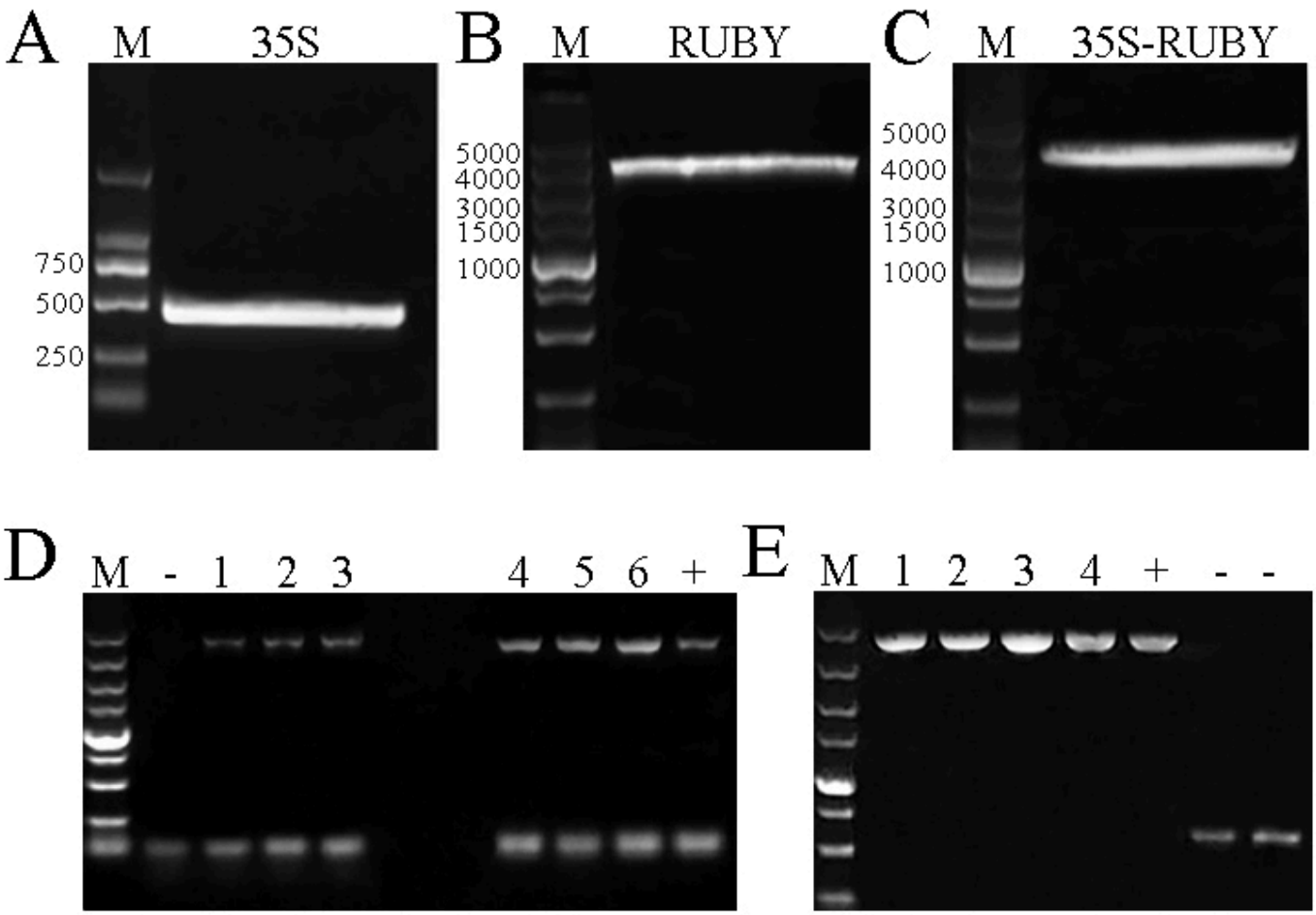

Figure 1

Legend not included with this version

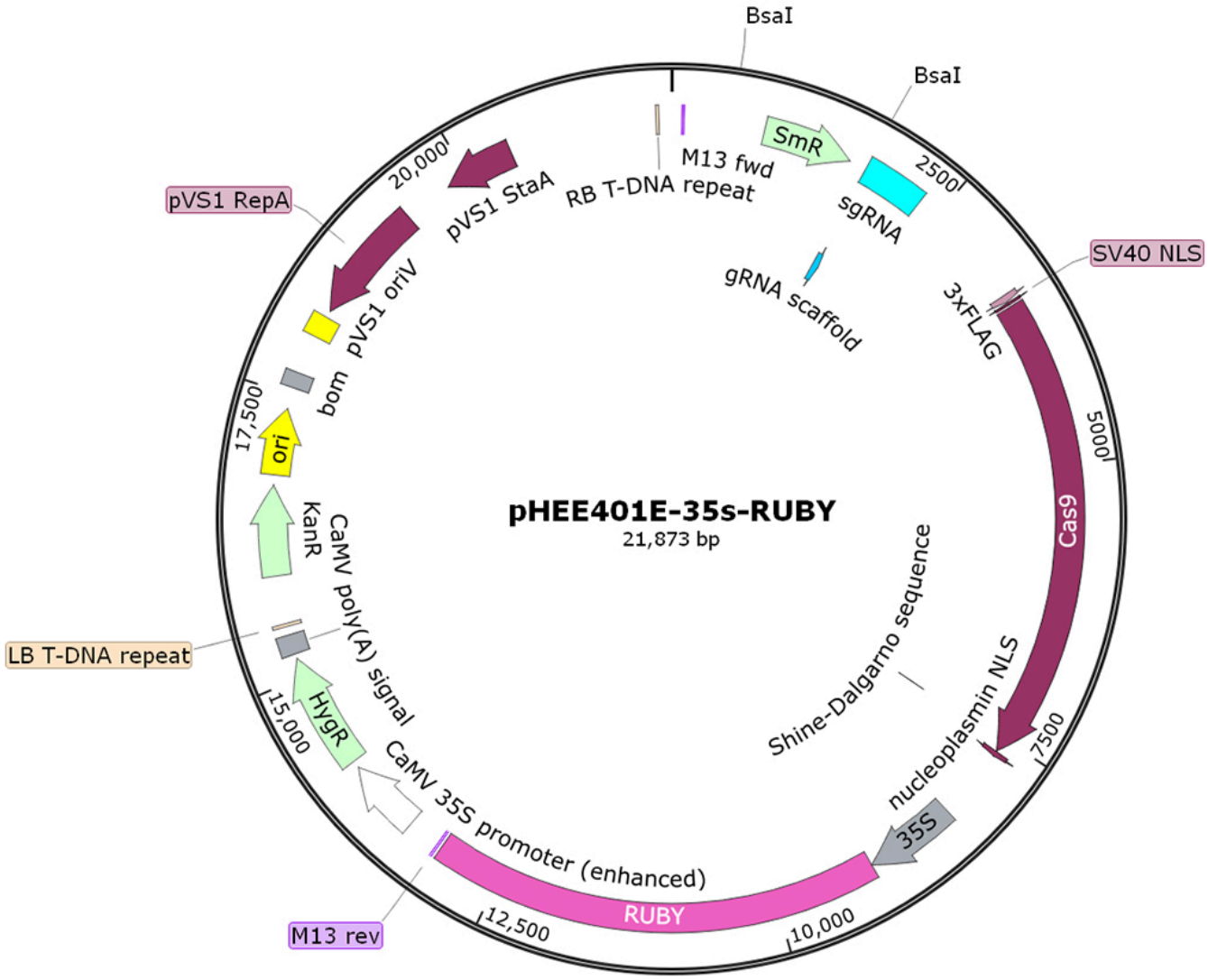

Figure 2

Legend not included with this version

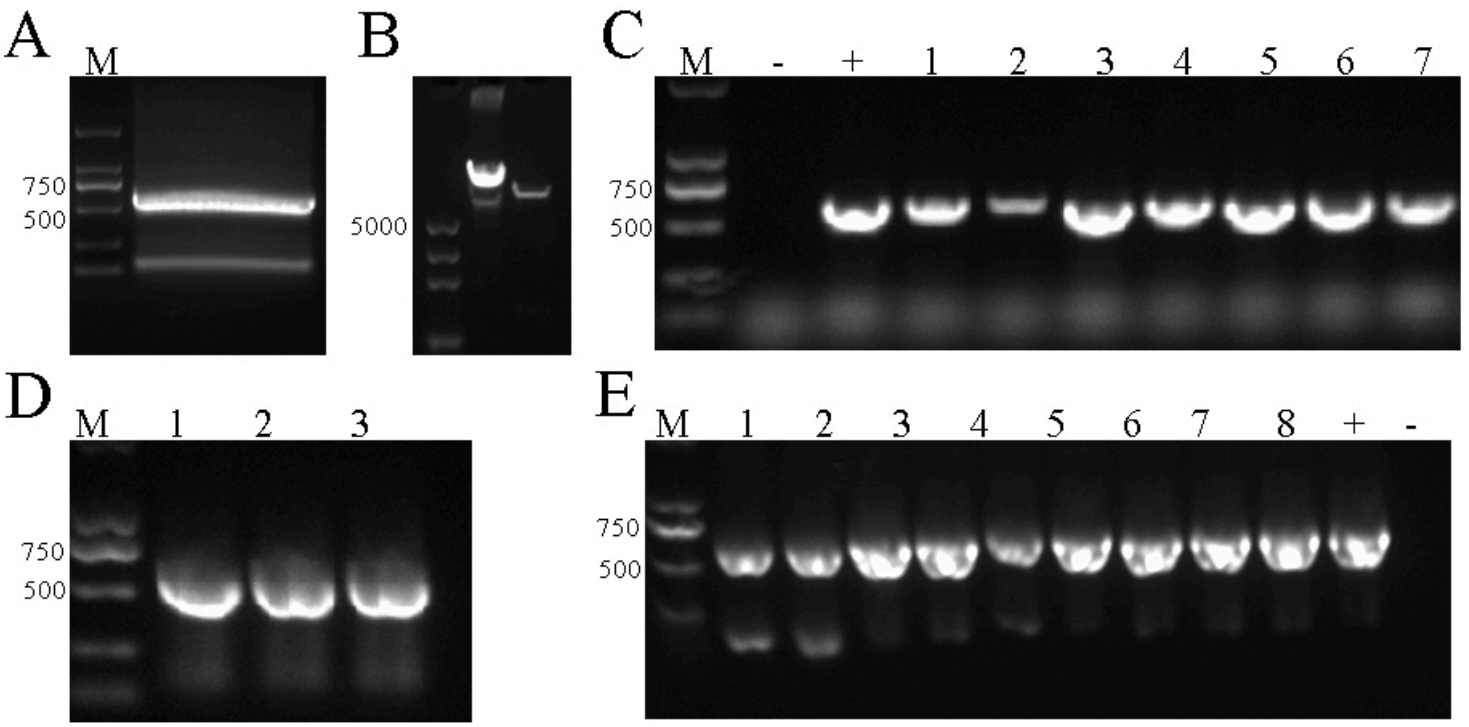

Figure 3

Legend not included with this version

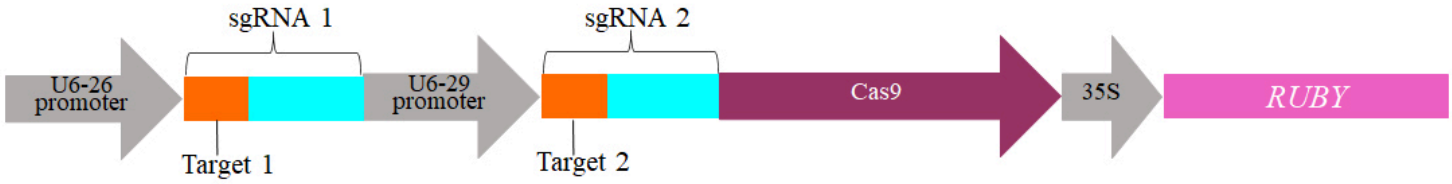

Figure 4

Legend not included with this version

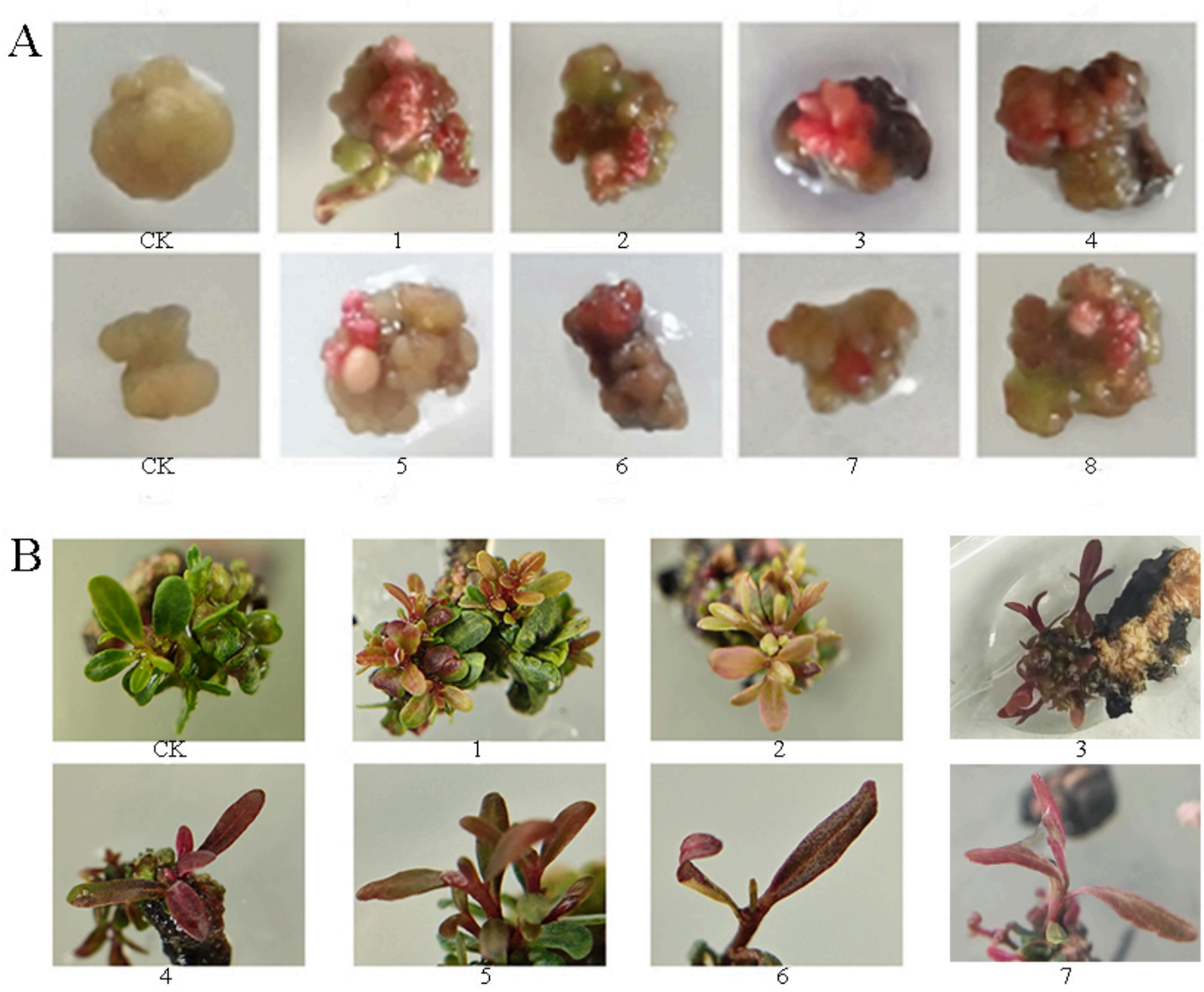

Figure 5

Legend not included with this version

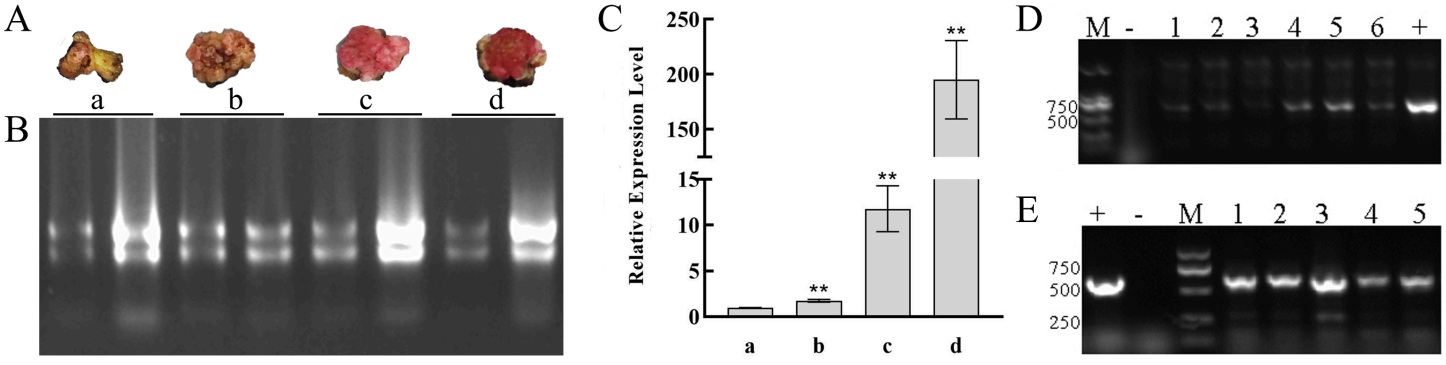

Figure 6

Legend not included with this version

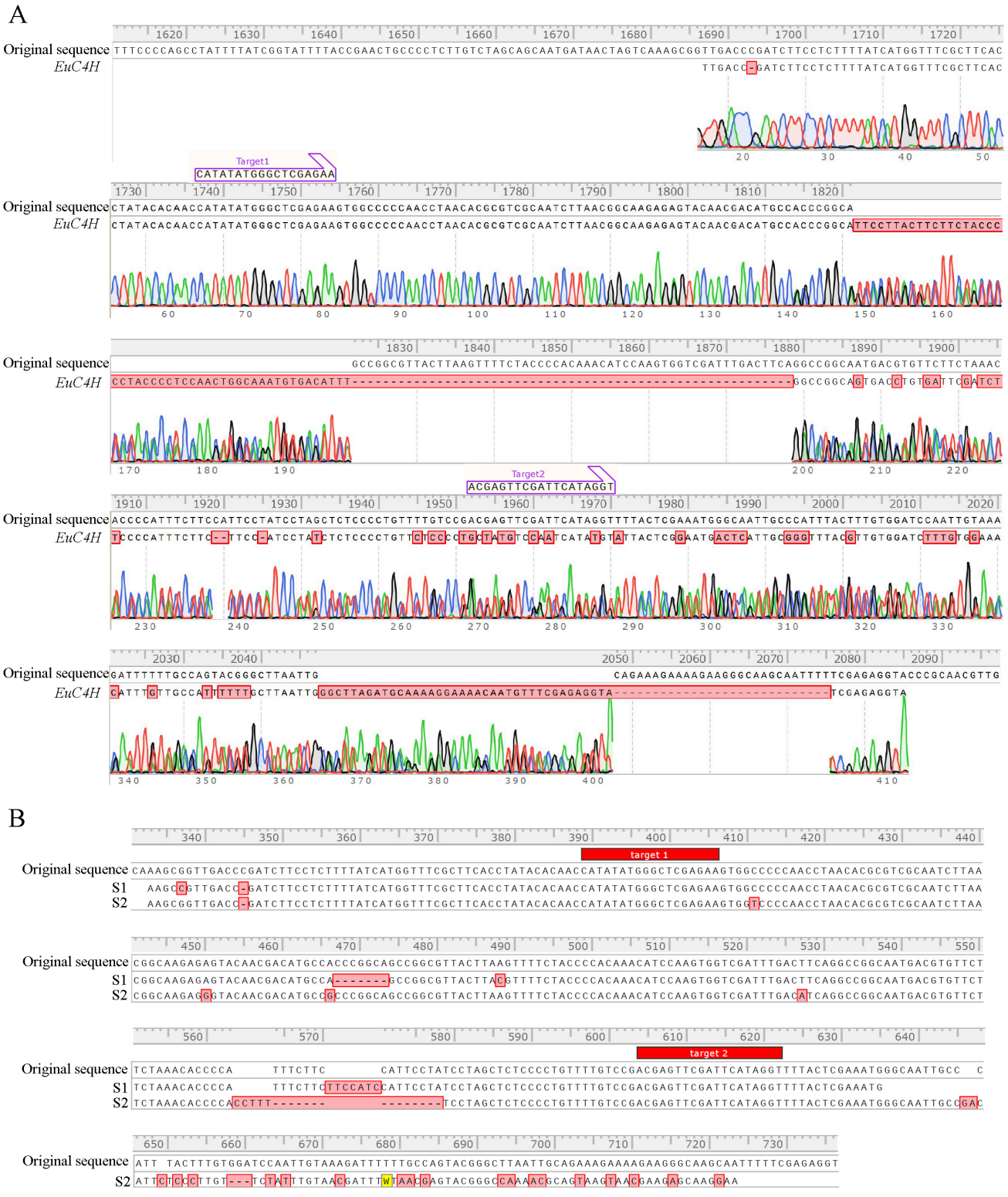

Figure 7

Legend not included with this version